

# Computational Processing and Detection of Mouse RGC from Ca Imaging Data

Shangjing Liu

Frank E Rodges Blvd North, Harrison, NJ 07029, United States

sl795@njit.edu

**Keywords:** RGC, Ca Imaging Data, Denoising.

**Abstract:** Mouse RGC experiment is a typical experiment. Electrophysiological method has always been a common method in neuroscience, and also used in this experiment. In recent years, calcium imaging of fluorescence indicators has also been widely used. In this article, we use a computational method to preprocess the mouse RGC experimental images of fluorescence, and identify the cell edge. Finally, we use fast Fourier transform on the typical cell response waveform.

## 1. Introduction

The development of vision restoration therapies is very slow. The progress of optoelectronics, photogenetics, gene therapy, and stem cell therapy[1-5] are all slow, because it is difficult to evaluate the effect of regeneration. Using Ca imaging to record the nerve cells in the intact eyeball can intuitively see the cells, which will promote the development of nerve cell regeneration experiments.

FACILE (functional adaptive optics cellular imaging in the living eye) in mouse[6] and monkeys[7] is a common method that combines high-resolution adaptive optics scanning light ophthalmoscopy(AOSLO)[8,9] and single cell calcium ion sensor genes coding[10]. Blocking the connection between central nervous system and brain activity to retinal nerve cells, by combining calcium imaging of fluorescence indicators, channelrhodopsin, and AOSLO, it is possible to effectively observe a large number of retinal nerve cells under experimental variable processing from optical images in vivo.

Ca imaging method can record calcium-dependent fluorescent sensors, which can form 1-100Hz images for recording nerve activity[11,12]. This optical imaging method can record thousands of cells in a period of time[13,14], from the sub-cell structure to the calcium ion activity of specific cells, thereby reflecting their nerve potential activity. Compared with electrophysiological methods, imaging methods can locate cells in tissues. As a result, the spatial localization enables post hoc characterizations in situ by immunohistology [15], cell-attached/whole-cell recordings [16,17], or electron-microscopy [18]. However, there are also many problems with the Ca imaging process. The main problem is that Ca imaging is to fluorescently label the calcium ion sensor of and record the intensity of the fluorescence sensor. This is an indirect way of responding to neural spiking. Fluorescence cannot perfectly and directly reflect the activity of the Ca sensor, and thus the response to the neural spiking during the recording period is not a perfect response[19]. In addition, the position movement caused by the motion of the experimental object during the recording process and the interference of the somatic cell signal on the fluorescence. For the processing of Ca imaging, the sensors are activated very quickly (50-200ms) but inhibited slowly (500ms-2s) after an action potential, this process is similar to a convolution process. So when responding to nerve impulses, use deconvolution to deal with the Ca imaging data can approximately get the time and intensity of the neural spiking[19]. However, in the Ca imaging experiment, under long-term light stimulation, the mouse RGC will have a difference in calcium ion concentration waveform. There are common activate waveforms that are similar to the convolution process, suppression waveforms that produce inhibitory potentials, and transients that act first and then inhibit or first inhibit and then act. In order to analyze the RGC in this experiment, this article performs fast Fourier transform on the waveform of the fluorescence intensity of Ca imaging cells over time.

## 2. Preprocessing of cell image

Due to the inevitable influence of various factors during the acquisition and transmission of the imaging process, the output inevitably has some noise. The noise will affect the original information, and it will have a significant impact on the image quality when calculating the amplitude. Noise can generally be removed by filtering, which is of great help to subsequent image processing.

### 2.1 Denoising

Image noise refers to the unnecessary or redundant information in the image like Fig.1, which is unpredictable and can only be recognized by statistical methods. Image noise is usually represented by digital features, mean variance or correlation functions, and its features can usually be reflected by these digital features.

### 2.2 Denoising Method

#### a. Average filter

The average filter is a typical linear filtering algorithm, which uses the the mean of domain. We replace the gray value of selected point by the target gray value. Let  $f(x,y)$  be the original image and  $g(x,y)$  be the averaged image, the formula is as follows:

$$g(x, y) = \frac{1}{n} \sum f(x, y)$$

$N$  is the number of pixels contained in the field.

Average filtering can remove the noise of the image well, while it can lose some details of the image, and the image will be blurred.

#### b. Median filter

The median filter is a non-linear digital filter technology that is often used to remove noise in pictures. The design idea is to check whether the sample of the input signal can represent the signal, use an odd number of observation windows to achieve this function, then the observation window at the median is the output, and discard the earliest value, obtain a new sample, and repeat the above operation.

$$f(x, y) = \text{mid}\{f(x \pm k, y \pm k), k \leq (n-1)/2\}$$

Median filtering is especially useful for speckle noise and salt and pepper noise, and it can maintain the sharpness of the edges.

#### c. Gaussian filter

Gaussian filter is a linear smoothing, which is suitable for eliminating Gaussian noise. Gaussian filtering is the process of weighted average of the entire image. The gray value of each pixel is obtained by weighted average of itself and other pixel values in the neighborhood.

$$g(x, y) = \frac{1}{2\pi\sigma^2} e^{-\frac{x^2+y^2}{2\sigma^2}}$$

## 3. Cell edge detection

Generally, we focus on the formed components of the cells. In order to obtain relevant information, the cells need to be separated from the background. Separating cells from time series data is not a small work. The definition of a good cell itself is a problem that needs attention. Generally speaking, we think that the bread-shaped round is the morphology of cells[21], but this definition is far from enough. When the cells are very close, it cannot be clearly identified.

For this problem, choosing different time series processing methods can be useful. Using the correlation map can make very close cell separation visible[22,23]. There are also many cells that are clearly visible in the average map, but are not clear in the correlation map, so more analysis is needed when processing these cells.

### 3.1 Convolutional neural networks

The edge of the image is one of the characteristics of the image, which plays an important role in the analysis of image recognition. Because of the discontinuity of the image edge, this feature can be used to segment the image in the process of image recognition.

In convolutional neural networks, we often use filter matrices to perform convolution operations on images, and identify the edges of the image through the feature map obtained by a specific convolution kernel.

### 3.2 Vertical and horizontal detection filters

When using vertical and horizontal detection filters, usually we use a 3\*3 matrix as a filter. The result of using this type of filter will detect the edge of the image horizontally or vertically. Combining the vertical detection and horizontal detection filters to obtain the horizontal and vertical edges of the image, the detected image edges can be obtained. Commonly selected filters are Roberts, Sobel, Prewitt and other operators (Fig.4), and their weights are different.

### 3.3 Thresholding

Thresholding is to select a threshold T, and divide the image into two parts, the background and the target, with T as the boundary. Suppose the grayscale image is f(x,y), the grayscale range is (0,L), find a suitable threshold T between 0 and L, and divide it into:

$$g(x,y) = \begin{cases} 1, & f(x,y) \geq T \\ 0, & f(x,y) < T \end{cases}$$

In thresholding method, how to choose the threshold determines the accuracy of segmentation. Common threshold segmentation methods include Otsu threshold segmentation method, adaptive threshold segmentation method, maximum entropy threshold segmentation method, iterative threshold segmentation method and so on.

In information theory, information entropy can explain the degree of chaos of a message, and the greater the entropy, the less clear the message. The definition of entropy is:

$$H(D) = -\sum_p p(x) \log p(x)$$

The use of image entropy as a criterion for image segmentation was proposed by Kapuret, which is still a widely used image entropy segmentation method[20].

Given a specific threshold  $q(0 \leq q < K-1)$ , for the two image regions  $C_0$  and  $C_1$  segmented by this threshold, the estimated probability density function can be expressed as :

$P_0(q)$  and  $P_1(q)$  respectively represent the cumulative probability of background and foreground pixels segmented by q threshold, and the sum of the two is 1. The entropy corresponding to the background and foreground is expressed as follows:

$$c_0: \left( \frac{p(0)}{P_0(q)}, \frac{p(1)}{P_0(q)}, \frac{p(2)}{P_0(q)}, \dots, \frac{p(q)}{P_0(q)}, 0, \dots, 0 \right)$$

$$c_1: \left( 0, \dots, 0, \frac{p(q+1)}{P_1(q)}, \frac{p(q+2)}{P_1(q)}, \dots, \frac{p(K-1)}{P_1(q)} \right)$$

$$P_0(q) = \sum_{i=0}^q p(i) = P(q)$$

$$P_1(q) = \sum_{i=q+1}^{K-1} p(i) = 1 - P(q)$$

$$H_0(q) = -\sum_{i=0}^q \frac{P(i)}{P_0(q)} \log \frac{P(i)}{P_0(q)}$$

$$H_1(q) = -\sum_{i=q+1}^{K-1} \frac{P(i)}{P_1(q)} \log \frac{P(i)}{P_1(q)}$$

Under this threshold, the total entropy of the image is:

$$H(q) = H_0(q) + H_1(q)$$

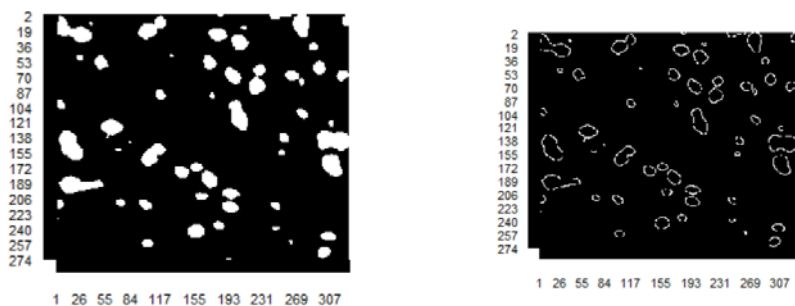
Calculate the total entropy of the image under all segmentation thresholds, find the maximum entropy, and use the segmentation threshold corresponding to the maximum entropy as the final

threshold. The pixels in the image whose grayscale is greater than this threshold are regarded as the foreground, otherwise as the background.

### 3.4 Thresholding result



(a) average map (b) The result of Convolutional neural networks



(c) The result of Otsu Method,  $T=0.33333$  (d) the result of Iterative thresholding,  $T=0.33326$

FIG.1 experimental results

From the experimental results (Fig.1b), the method of edge detection using convolution operator is not good. Since we use the fluorescence method to reflect the changes in the concentration of Ca in the cells, the gray value of the resulting image has good continuity, and there are few edge mutations, so the convolution operator does not detect the edges of cells well. Furthermore, since the gray value change is at the peak at the center of the cell, the center of the cell will be displayed as an "edge", so we do not use the convolutional neural network method here.

### 4. Conclusion

This article deals with the processing of time series data of Ca images in mouse RGC experiments. We focus on preprocessing of image noise, cell segmentation and recognition, and Fourier transform of cell fluorescence intensity waveform under time series. In these discussions, there have been many mature steps in the preprocessing of noise, the generation and types of noise, and the processing methods for them. There are also different kinds of methods for cell segmentation and recognition. But we deal with images that reflect the concentration of calcium ions, which existence in cells has continuity, as well as the complexity of the background, these all lead to the use of edge detection is not suitable here. This article uses the threshold method for segmentation, which can better segment the background and cells.

However, due to the complexity of the background again, even if the threshold method is used for segmentation, there will still be redundant information generated by the background. In addition, some cells have very weak responses. If the threshold is too low, the cell information will also be deleted, so the image is segmented in combination with morphology. Due to the threshold method, for cells that are very close or even overlapped, the threshold method cannot well divide the boundaries between such cells. In this article, because the cell's response type and time are different, the fluorescence intensity peak is different, so different time thresholds are used to separate such cells.

Finally, a brief introduction of Fourier transform and fast Fourier transform of cell waveforms of typical response types are briefly presented. However, due to the complexity of the waveform itself,

how to use the fast Fourier transform results to describe the speed of the induction peaks, the speed of the troughs, the speed of the peaks falling back, the speed of the peaks and troughs rising, etc., are not analyzed in detail in this article.

## References

- [1] Fine I, Cepko CL, Landy MS. Vision research special issue: Sight restoration: Prosthetics, optogenetics and gene therapy. *Vision Res.* 2015; 111(Pt B):115–23. <https://doi.org/10.1016/j.visres.2015.04.012> PMID: 25937376.
- [2] Theogarajan L. Strategies for restoring vision to the blind: current and emerging technologies. *Neurosci Lett.* 2012; 519(2):129–33. <https://doi.org/10.1016/j.neulet.2012.02.001> PMID: 22414860.
- [3] Garg SJ, Federman J. Optogenetics, visual prosthesis and electrostimulation for retinal dystrophies. *Curr Opin Ophthalmol.* 2013; 24(5):407–14. <https://doi.org/10.1097/ICU.0b013e328363829b> PMID: 23799487.
- [4] Scholl HP, Sahel JA. Gene therapy arrives at the macula. *Lancet.* 2014; 383(9923):1105–7. [https://doi.org/10.1016/S0140-6736\(14\)60033-7](https://doi.org/10.1016/S0140-6736(14)60033-7) PMID: 24439295.
- [5] O'Brien EE, Greferath U, Vessey KA, Jobling AI, Fletcher EL. Electronic restoration of vision in those with photoreceptor degenerations. *Clin Exp Optom.* 2012; 95(5):473–83. <https://doi.org/10.1111/j.1444-0938.2012.00783.x> PMID: 22823954.
- [6] Yin L, Geng Y, Osakada F, Sharma R, Cetin AH, Callaway EM, et al. Imaging light responses of retinal ganglion cells in the living mouse eye. *J Neurophysiol.* 2013; 109(9):2415–21. <https://doi.org/10.1152/jn.01043.2012> PMID: 23407356; PubMed Central PMCID: PMC3652215.
- [7] Yin L, Masella B, Dalkara D, Zhang J, Flannery JG, Schaffer DV, et al. Imaging light responses of foveal ganglion cells in the living macaque eye. *J Neurosci.* 2014; 34(19):6596–605. <https://doi.org/10.1523/JNEUROSCI.4438-13.2014> PMID: 24806684; PubMed Central PMCID: PMC4012315.
- [8] Liang J, Williams DR, Miller DT. Supernormal vision and high-resolution retinal imaging through adaptive optics. *J Opt Soc Am A Opt Image Sci Vis.* 1997; 14(11):2884–92. PMID: 9379246.
- [9] Roorda A, Romero-Borja F, Donnelly W Iii, Queener H, Hebert T, Campbell M. Adaptive optics scanning laser ophthalmoscopy. *Opt Express.* 2002; 10(9):405–12. PMID: 19436374.
- [10] Chen TW, Wardill TJ, Sun Y, Pulver SR, Renninger SL, Baohan A, et al. Ultrasensitive fluorescent proteins for imaging neuronal activity. *Nature.* 2013; 499(7458):295–300. Epub 2013/07/23. <https://doi.org/10.1038/nature12354> PMID: 23868258; PubMed Central PMCID: PMC3777791.
- [11] Helmchen F, Denk W: Deep tissue two-photon microscopy. *Nature Methods* 2005, 2:932.
- [12] Grienberger C, Konnerth A: Imaging calcium in neurons. *Neuron* 2012, 73:862-885.
- [13] Ahrens MB, Orger MB, Robson DN, Li JM, Keller PJ: Whole-brain functional imaging at cellular resolution using light-sheet microscopy. *Nature Methods* 2013, 10:413.
- [14] Stringer C et al.: Spontaneous behaviors drive multidimensional, brain-wide population activity. *bioRxiv* 2018. URL: <https://www.biorxiv.org/content/early/2018/04/22/306019.full.pdf>
- [15] Khan AG, Hofer SB: Contextual signals in visual cortex. *Current Opinion in Neurobiology* 2018, 52:131-138.

- [16] Znamenskiy P et al.: Functional selectivity and specific connectivity of inhibitory neurons in primary visual cortex. *bioRxiv* 2018:294835.
- [17] Weiler S et al.: High-yield in vitro recordings from neurons functionally characterized in vivo. *Nature Protocols* 2018, 13:1275.
- [18] Bock DD et al.: Network anatomy and in vivo physiology of visual cortical neurons. *Nature* 2011, 471:177.